Residual Stress and Magnetic Properties of Nickel, Cobalt, Iron and FeCo Electrodeposits

S, Kelcher[1], D.-Y. Park[2], and N. V. Myung[1,]*
[1]Department of Chemical and Environmental Engineering, University of California-Riverside, Riverside, CA 92521
[2]Department of Applied Materials Engineering
Hanbat National University, San 16-1, Dukmyung-dong
Yuseong-gu, Daejon, 305-719, South Korea

Nano-/Micro-ElectroMechanical Systems (NEMS/MEMS) devices including microactuators, sensors, micromotors, and frictionless microgears, spintronic devices, nanowires and nanorods use magnetic materials because electromagnetically-actuated NEMS/MEMS are more stable for high force and large actuation gap applications.

In order to integrate magnetic materials to MEMS/NEMS, physical properties (e.g. film stress, magnetic and electric properties, corrosion resistance) and deposition processes (e.g. operating temperature, pH) must be "tailored". Especially, good magnetic properties with minimum residual stress are essential for magnetic materials for successful integration to magnetic-NEMS/MEMS. In the present studies various low-stress iron group metals and FeCo alloy thin films were developed. The effect of deposition parameters on film compositions, surface morphology, magnetic properties and residual stress of electrodeposits were investigated using scanning electron microscopy (SEM), flexible strip method, and vibrating sample magnetometer (VSM). In general, low stress iron group metals and FeCo alloys were electrodeposited by applying low current density (e.g. 5 mA cm^{-2}) and high operating temperature (e.g. $70^{O}C$) in an acidic chloride bath. Magnetic properties including coercivity (H_C) and squareness (M_R/M_S = remanence/magnetic saturation) were strongly influenced by residual stress.

For more information contact:
Prof. Nosang V. Myung
Bourns Hall B353
University of California-Riverside
Riverside, CA 92521
Phone: (909)827-7710
FAX: (909)787-5696
E-mail:myung@engr.ucr.edu

INTRODUCTION

The ever-increasing demands for faster, smaller and less expensive electronic systems, such as integrated circuits (ICs), microelectromechanical systems (MEMS) and computer hard disk drives (HDDs), have resulted in the development of cost-effective processes. The incredible increased speeds of the aerial density of HDDs (100 % per year) is a good example of current trend in this technology. To meet this strong demand for HDDs, soft magnetic materials with high magnetic saturation (M_S) are intensively being investigated by several research groups [1].

In the case of MEMS, hard and soft magnetic materials are used in microactuators, sensors, micromotors, and frictionless microgears because electromagnetically-actuated MEMS are more stable for high force and large gap applications. These are more robust in harsh environments (dust, humidity), and can be actuated with low cost voltage controllers [2-7].

There are many different ways to deposit and integrate magnetic materials into magnetic-NEMS/MEMS including vacuum deposition (i.e. sputtering, e-beam evaporation, chemical vapor deposition, molecular beam epitaxy) and electrochemical deposition (i.e. electrodeposition, and electroless deposition). Compared to vacuum processes, electrochemical processing is well-suited to fulfill the requirement of high yield and cost-effective processes.

Electrochemical processes have many advantages, including precisely controlled room temperature operation, low energy requirements, rapid deposition rates, capability to handle complex geometries, low cost, and simple scale-up with easily maintained equipment. In addition, the properties of materials can be "tailored" by controlling solution compositions and deposition parameters. Due to these advantages, electroplated soft magnetic materials such as NiFe and CoNiFe have been widely used as recording head materials by computer hard drive industries [8]. In the case of magnetic-MEMS/NEMS, the magnetic layer thickness can vary from a few nanometers to a few millimeters depending on the application. Magnetic thin films must also have good adhesion, low-stress, corrosion resistance, and be thermally stable with excellent magnetic properties.

Even though there are many studies on electrodeposited iron group metals and alloys, there is a lack of systematic studies relating magnetic properties with residual stress and deposit compositions. In this paper, we investigated and compared the effect of solution compositions and electrodeposition parameters on the nature of the films in terms of their compositions and structure, stress, and magnetic properties.

EXPERIMENTAL

Nickel, iron, cobalt and FeCo alloys were electrodeposited from various plating solutions listed in table 1. Calcium chloride was used as the supporting electrolyte to enhance the current efficiency. Solution pH was adjusted between 0.3 and 0.4 with HCl or NaOH. Experiments were conducted at different operating temperatures (room temperature to 70°C) with no stirring. The effect of the solution Fe^{+2}/Co^{+2} ratio on the deposit composition of FeCo alloy films was investigated by varying the Fe^{+2} and Co^{+2} concentration with total iron group metal ions set at 1.5 M. Cu-Be substrate with surface areas of 7.74 cm^2 were used: Fe, Co, or Ni were used as

soluble anodes for the alloy baths. Current density was varied from 2.5 to 60 mA cm^{-2} with a fixed total charge of 60 Coulomb. Surface morphology and film compositions were examined using SEM and EDS, with a known standard, respectively. Magnetic properties of electrodeposited films were measured with a vibrating sample magnetometer (Lakeshore 735). Film stress was measured with a flexible strip method [9].

Table 1. Solution Compositions of nickel, cobalt, iron and FeCo alloys.

Ni	1.5 M $NiCl_2$ + 1.0 M $CaCl_2$
Co	1.5 M $CoCl_2$ + 1.0 M $CaCl_2$
Fe	1.5 M $FeCl_2$ + X M $CaCl_2$ (X = 0, 0.25, 1.0)
FeCo	Y M $FeCl_2$ + (1.5-Y) M $CoCl_2$ + 1.0 M $CaCl_2$ (Y = 0 to 1.5 M)

RESULTS AND DISCUSSION

In the case of magnetic-NEMS/MEMS, the shapes, structures, and functionality can be very different depending on the application. Figures 1 shows a few examples of authors' previous NEMS/MEMS devices with integrated electrodeposited materials. Figure 1a & b show the micro force-detected nuclear magnetic resonance (μFD-NMR) to identify chemical compounds for in-situ planetary exploration and nickel nanowires for biomedical applications, respectively. Figure 1c & d show the LIGA fabricated scroll pump for vacuum roughing pump and the two-dimensional 3 X 3 quadrupole mass filter, respectively, for miniaturized gas chromatograph/mass spectrometer (GC/MS). As shown in figures, the layer thickness can vary from a few nanometers to a few millimeters depending on the applications. In addition, the magnetic materials and deposition processes must be "tailored" to be compatible with other MEMS processing including photo-resistive patterning, vacuum deposition, and chemical and physical etching.

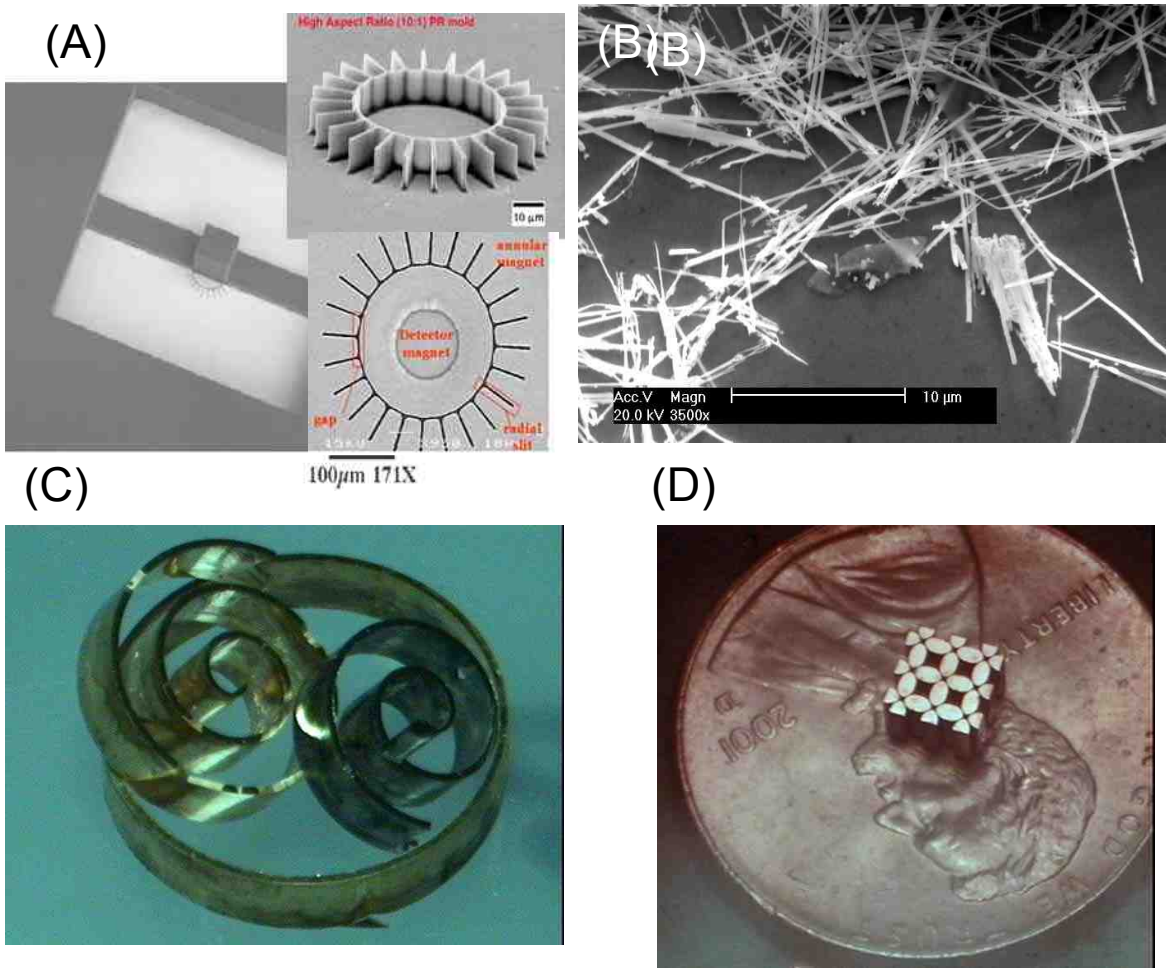

Figure 1. A few examples of electrodeposited MEMS devices; (A) micro-force detector Nuclear Magnetic Resonance (μFD-NMR): (B) Electrodeposited nickel nanowires with diameter of 200 nm: (C) Miniature Vacuum Roughing Pump: (D) Miniaturized Two-Dimensional Quadrupole Mass Filter for Micro GC/MS instrument.

Electrodeposited Nickel, Cobalt and Iron Films

Figure 2 and 3 shows the dependence of film stress, magnetic properties (i.e. coercivity and squareness) of electrodeposited nickel and cobalt films as a function of current density at a fixed temperature of 66-68°C. Residual stress in the electrodeposited films is an important factor for MEMS using LIGA processes. In many cases, this film stress could exceed the strength of the film, resulting in cracking, deformation of devices, and interfacial failure. As shown in figure 2a and 3a, the residual stress of electrodeposited nickel and cobalt films increased monotonically as current density increased. For example, electrodeposited nickel and cobalt film'stress increased from 70 MPa to 202 MPa and from 105 MPa to 202 MPa with an increase in deposition current density from 2.5 mA cm^{-2} to 60 mA cm^{-2}, respectively.

Magnetic saturations (M_S) of electrodeposited nickel and cobalt films were 0.6 T and 1.8 T, respectively, independent of electrodeposition conditions and followed bulk data as expected. Coericivity (H_C) (*i.e.* a quantitative measure of the magnetic field required to reverse the magnetization direction in the film) and squareness ($S = M_R/M_S$) (*i.e.* the remnant magnetization force after the magnetic field was reduced to zero) were dependent on the deposition conditions since they are extrinsic magnetic properties which were dependent on the film microstructure, including grain size, preferred orientation, and stress. As shown in Figure 2b, the coercivity of electrodeposited Ni films increased with increasing film stress, which indicates that magnetoelastic energy was the dominant anisotropy energy in the electrodeposited Ni films. Squareness was decreased, as expected from the literature, since tensile stress causes a magnetic curve to be less square when magnetoelastic energy is the dominant anisotropy energy (figure 2c). Unlike electrodeposited nickel films, there were no clear relationships between coericivity and residual stress in electrodeposited cobalt films, which indicated that magnetoelastic energy is not a dominant anisotropy energy (figure 3b). In contrast to electrodeposited nickel films, squareness increased with increasing residual stress in such cobalt films (figure 3c).

Figure 4 shows the dependence of film stress, magnetic properties (*i.e.* coercivity and squareness) of electrodeposited iron films as a function of current density at a fixed temperature of 66-68 °C. Residual stress iron electrodeposits increased monotonically as current density was increased. For example, electrodeposited iron film stress increased from 120 MPa to 240 MPa with an increase in deposition current density from 5 mA cm^{-2} to 20 mA cm^{-2}, respectively. Magnetic saturations (M_S) of electrodeposited iron films were 2.1 T independent of electrodeposition conditions. As shown in Figure 4b, the coericivity of electrodeposited iron films increased with increasing film stress, which indicates that magnetoelastic energy was the dominant anisotropy energy. Squareness was decreased in electrodeposited nickel films, since tensile stress causes a magnetic curve to be less square when magnetoelastic energy is the dominant anisotropy energy (figure 4c).

Figure 5 shows the SEM micrographs of electrodeposited iron films at different current density (5, 10, and 20 mA cm^{-2}) at $50^{O}C$. As shown in these figures, surface morphologies for Fe films influenced deposition temperature. Low current density promoted grain growth, while high current densities promoted nucleation and produces smaller grains. Higher deposition temperature (i.e. $70^{O}C$, not shown in figure) promoted larger grain growth than lower deposition temperatures.

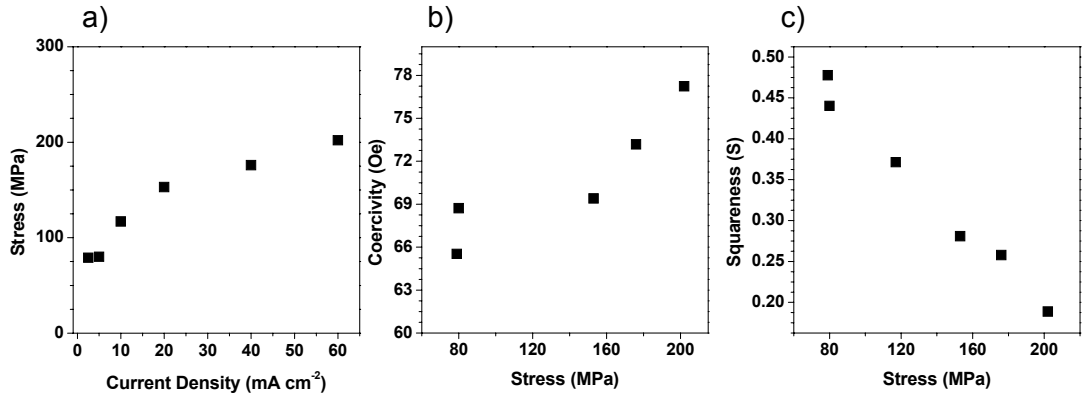

Figure 2. Residual stress (a), coericivity (b), and squareness (remenance(M_R)/magnetic saturation (M_S)) (c) of electrodeposited Ni films as a function of current density. Solution pH and operating temperature were 0.3 and 70^{O}C, respectively.

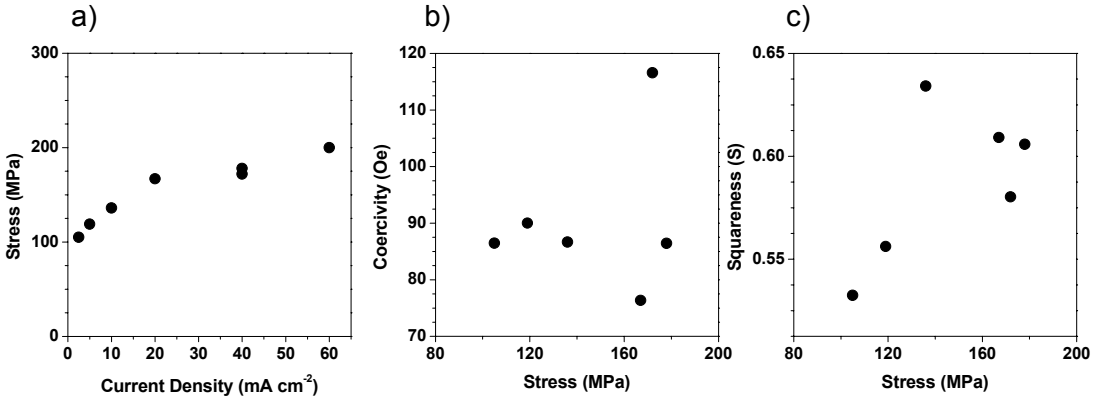

Figure 3. Residual stress (a), coericivity (b), and squareness (remenance(M_R)/magnetic saturation (M_S)) (c) of electrodeposited cobalt films as a function of current density. Solution pH and operating temperature were 0.3 and 70^{O}C, respectively.

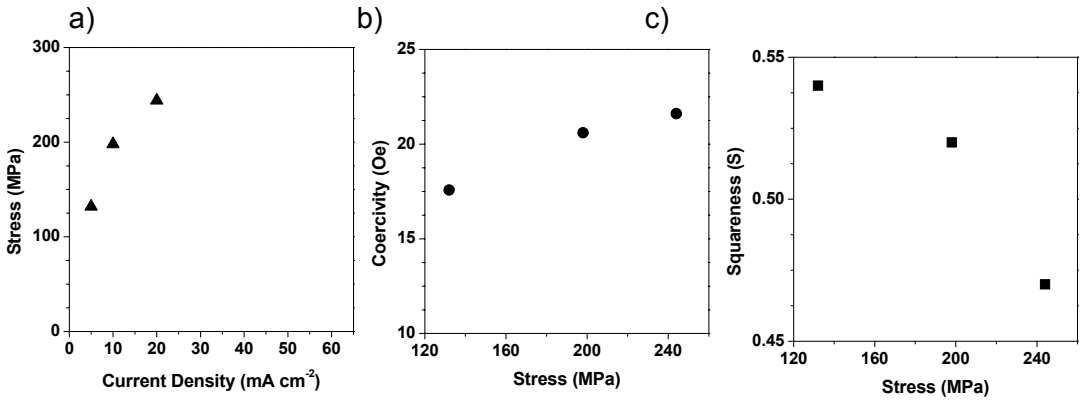

Figure 4. Residual stress (a), coericivity (b), and squareness (remenance(M_R)/magnetic saturation (M_S)) (c) of electrodeposited iron films as a function of current density. Solution pH and operating temperature were 0.3 and 70^{O}C, respectively.

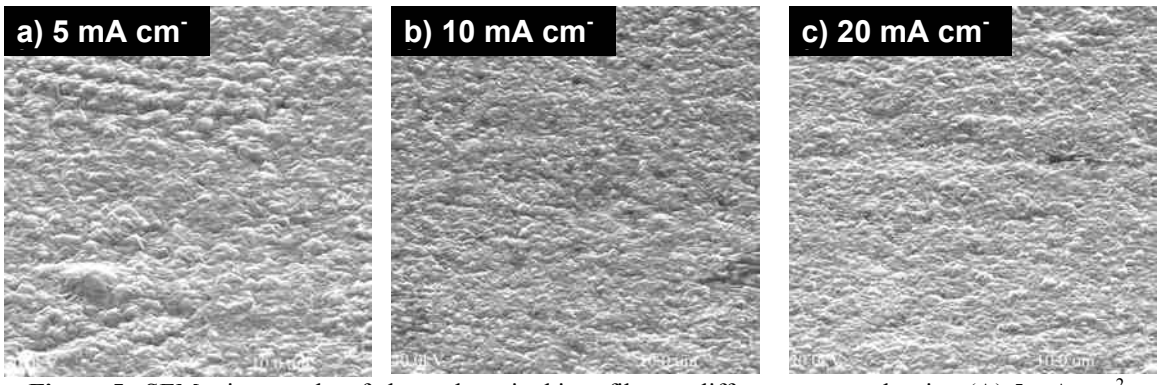

Figure 5. SEM micrographs of electrodeposited iron films at different current density; (A) 5 mA cm^{-2}, (B) 10 mA cm^{-2}, and (C) 20 mA cm^{-2}: Temperature = 70^{O}C.

Electrodeposited FeCo Films

Difference film composition of FeCo alloy thin films were electrodeposited by varying the solution Fe^{+2}/Co^{+2} ratio while maintaining the total iron group metal ions constant at 1.5 M. Figure 6 shows the deposit Fe content (a) and residual stress (b) as a function of solution compositions at various current densities. As shown in figure 5a, deposit Fe contents increased with increasing Fe^{+2}/Co^{+2} ratio as expected. Maximum residual film stress of FeCo thin films were observed from FeCo thin film with deposit Fe content of 5 to 10 atomic percent.

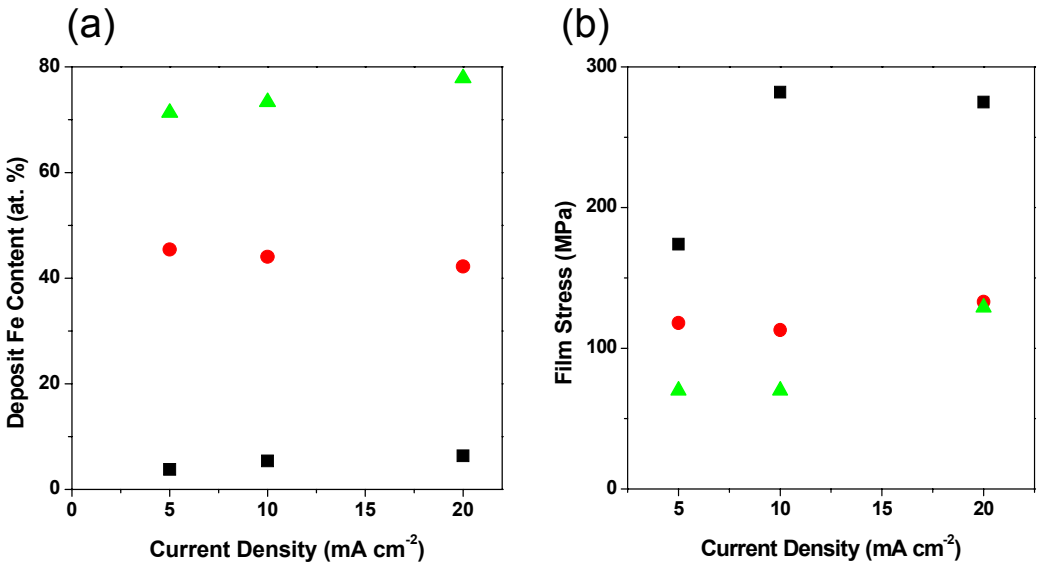

Figure 6. Deposit Fe content and film stress as a function of solution composition at different current densities (5 to 20 mA cm^{-2}). ■ 0.15 M Fe^{+2} + 0.135 M Co^{+2}; ● 1.05 M Fe^{+2} + 0.45 M Co^{+2}; ▲ 1.275 M Fe^{+2} + 0.125 M Co^{+2}. Operating temperature = 70^{O}C.

Figure 7 shows SEM micrographs of electrodeposited FeCo films with different film compositions at a CD of 5 mA cm^{-2}. As shown in the images, surface morphology of FeCo films dramatically changed with FeCo film compositions. FeCo grain size increased with an increase in deposit Fe content, where small grain was observed in the 3.8Fe96.2Co films (Figure 6.b).Residual film stress of FeCo films decreased with increase in grain size. An earlier report [10] had also demonstrated that electrodeposited mixed phase FeCo alloys produced films with smaller grain size. Magnetic saturation of FeCo alloys increased with increasing in deposit Fe content. For example, magnetic saturation of 1.6 T, 1.9T, and 2.0T were measured from FeCo electrodeposits with deposit Fe content of 3.8 %, 35.1%, and 45.4%.

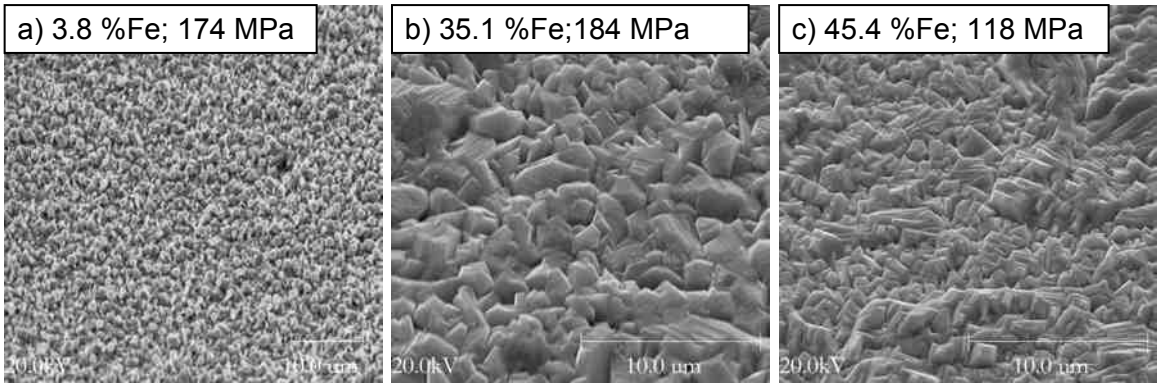

Figure 7. SEM micrographs of electroformed FeCo films; (A) 3.8 % Fe, (B) 35.1 %Fe, (C) 45.4 % Fe: CD = 5 mA cm^{-2} and Deposition Temperature = 66-68°C.

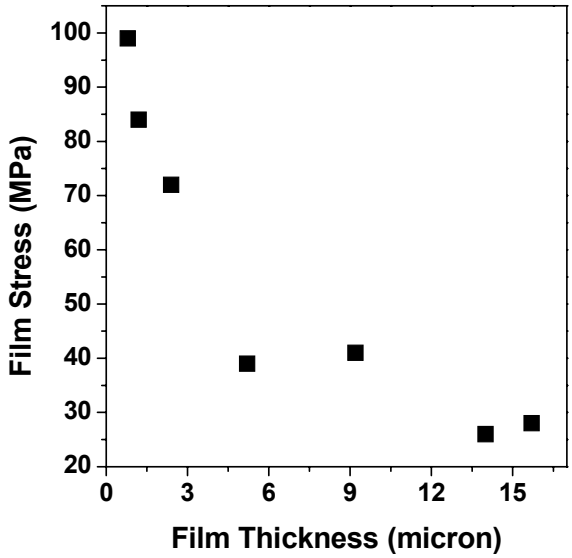

Figure8. Residual stress of FeCo electrodeposits as a function of film thickness: FeCo film were electrodeposited from 1.275M FeCl2+0.225M CoCl2+1.0M CaCl2; pH = 0.3; Temp. = 70 ^{O}C.

Figure 8 shows the residual stress of FeCo films as a function of film thickness. As expected, the residual stress decreased with increasing film thickness. High initial stress is attributed to lattice and grain size mismatch between deposits and the underlying substrate [9]. Residual stress decreased to steady state value as the deposit increased in thickness.

CONCLUSION

Electrodeposition of nickel, cobalt, iron and FeCo alloys thin film were investigated from additive-free acidic chloride baths with calcium chloride as a supporting electrolyte. In general, low film stress was achieved by operating at a low current density and higher temperature. SEM micrographs indicate that these conditions promote grain growth over nucleation. Magnetic properties including coercivity and squareness were strongly influenced by residual stress. Coercivity in electrodeposited nickel and iron films increased with increasing residual stress while sqaureness decreased, indicating that magnetoelastic energy was a dominant anisotropy in electrodeposited nickel and iron films. No trends were observed in electrodeposited cobalt films, which indicate that other anisotropy energies (e.g. crystal anisotropy) are dominant.. In the case of FeCo thin films, film compositions play an important role in residual stress.

REFERENCES

1. T. Osaka, M. Takai, K. Hayashi, K. Ohashi, M. Saito, and K. Yamada, *Nature*, **392**, 796-798 (1998),
2. T. S. Chin, *J. Magn. Magn. Mater*. **209** , 75-79 (2000).
3. J. W. Judy and R. S. Muller, *IEEE J. Microelectromechanical Sys*., **6**(3), pp. 249-256, (1997).

4. J. W. Judy and R. S. Muller, Sensors and Actuators (Physical A), **A53**, 392-397 (1996).
5. J. W. Judy, R. S. Muller and H. H. Zappe, IEEE J. Microelectromechanical Systems, **4**(4), 162-69 (1995).
6. C. H. Ahn and M. G. Allen, *IEEE Trans. Ind. Electron.* **45**(6), 866-876 (1998).
7. T. M. Liakopoulos, M. Xu and C. H. Ahn, Technical Digest Solid-State Sensor and Actuator Workshop, Hilton Head Island, SC, USA, 19-22 (1998).
8. P. C. Andricacos and N. Robertson, *IBM J. Res. Develop*., **42**(5), 671-80 (1998).
9. J. W. Dini, "Electrodeposition, The Material Science of Coating and Substrates", Noyes Publications, p. 292 (1992).
10. N. V. Myung and K. Nobe, *J. Electrochem. Soc.*, **148**, C136 (2001).

